ICAS 2021 SHANGHAI
International Council of the Aeronautical Sciences
32nd Congress of the International Council of the Aeronautical Sciences
September 6-10, 2021
Pudong Shangri-La, Shanghai, China

EXPERIMENTAL STUDIES OF SLOT-TYPE CASING TREATMENTS FOR MODEL FANS WITH THE AIM OF AERODYNAMIC AND ACOUSTIC IMPROVEMENTS

V. Mileshin [1], S. Markov [1], V. Korzhnev[1], Ia. Pochkin[1]

[1] Central Institute of Aviation Motors (CIAM), 111116, Moscow, Aviamotornaya, 2

Abstract

In developments of conventional and counter-rotating fans for advanced new-generation aircraft engines with ducted blades, it is very important to ensure high aerodynamic and acoustic characteristics. This work presents experimental studies of aerodynamic and acoustic characteristics for the models of C179-2 single-row fan and the CRTF2A counter-rotating fan with versions of slot-type casing treatments (CT) installed. The CRTF2A counter-rotating fan was designed, manufactured and tested at CIAM C-3A test facility under the European VITAL project. The CRTF2A counter-rotating fan was equipped with the turbulence control screen (TCS).

Nine versions of two-row slot-type casing treatments as applied to the CRTF2A counter-rotating fan were tested. As a result of the experimental data analysis from aerodynamic tests with the aim to study the effect of shapes and relative positions of slots in the CTs as well as the CT height on key CRTF aerodynamic characteristics, it is found that:

All tested CTs considerably improves the fan stall margins (from 4.9 % to 8.9 %) in medium and high operating conditions (n=75–100 %). The increase in stall margins at n=54 % is from 10 % to 22 %.

Relative position of slots in the two-row CT with the same number of slots in both rows has a noticeable effect on the CT efficiency. A shift of axes of the slots relative to each other by half a pitch leads to a slight increase (by max. 1.6 %) in stall margins in medium and high operating modes and a noticeable increase (by 2%) in efficiency in the same modes, except for n=100 %.

Analysis of experimental acoustic characteristics for 3 CT two-row configurations, as applied to the CRTF2A counter-rotating fan model, shows that a decrease in the acoustic power is nearly the same for these three CT configurations in three certification modes. The overall decrease in the acoustic power in three certification modes for the CRTF2A fan model with the two-row CT installed over the second rotor is 3.2–3.5 dB.

In addition to a considerable improvement in gasdynamic characteristics of the C179-2 single-row bypass fan, the use of this type CTs for the model stage in the C179-2 single-row by-pass fan substantially improves its acoustic characteristics. The overall decrease in the acoustic power in three certification modes for the C179-2 single-row by-pass fan is 3 dB.

Keywords: fan model, casing treatment, surge margin, sound pressure

1. Nomenclature

CT	Casing treatment;
CDP	Cruise design point;
IGV	Inlet Guide Vane
G_{cor}	corrected mass flow rate
$\bar{n}_{cor}$	corrected rotational speed
ΔSM	Surge margin
U_{tip}	tip speed of a fan blade leading edge, m/s
Ps	static pressure, kPa
Pt	total pressure, kPa
Tt	total temperature, C
π^*	total pressure ratio of the fan model
π^*/π^*_{CDP}	total pressure ratio / total pressure ratio at a design point
$\eta^*_{ad}/\eta^*_{ad.CDP}$	adiabatic efficiency / adiabatic efficiency at a design point
h	CT slot height in mm or a blade height, mm
δs	slot width in circumferential direction, mm
ts	slot cascade pitch, mm
I	core duct
II	bypass duct
cor	corrected

2. Introduction

Developments of specific procedures for the purpose of higher compressor stall margins took its origin in 1950s when an increase in pressure in GTE compressors and operating conditions associated with flow disturbances at the compressor inlet became more complicated. At the same time, along with such classical methods of compressor control as variable stator vanes and air bleed, casing treatments not requiring forced control and designed to prevent local flow separations on blades were developed [1, 2].

Benefits of slot-type CTs in increasing stall margins, efficiency and improving acoustic characteristics were shown in [3, 4].

The complexity of flow in compressors, especially in the flow stalled area, its spatial nature with high vorticity and unsteadiness as well as viscosity, have not allowed yet to propose a closed procedure for CT aerodynamic computations and designing.

As of today, a great number of works has been published devoted to a detailed study of 3D viscous unsteady flow in stages of axial compressors with CTs of various types, which are focused on various aerodynamic aspects of the CT effect on flow [5-15].

This paper describes an efficient CT designed at CIAM, sets forth physical foundations of the CT functioning, and presents generalized results of experimental studies. The completed study was aimed not only the CT effect on aerodynamics, but also on acoustic characteristics of fans and compressors.

Conventional CTs developed by CIAM have one uniform slot section. In 2016 first CTs were designed and manufactured for the CRTF1 counter-rotating fan model, produced under the European VITAL program [16-18]. In October 2016, aerodynamic and acoustic tests of the CRTF1 fan with these CTs were completed at the C-3A test facility that showed their high aerodynamic and acoustic efficiency [19].

In 2017, modified CTs were designed and manufactured for the same CRTF1 fan; they had two slot sections located one after another and united by one common cavity. In addition to high aerodynamic characteristics, i.e. efficiency and stall margins, all configurations of those CTs provided a steady reduction in fan model noise in key certification modes [20].

In 2018, a new combined CT was developed and manufactured for the C179-2 single-row bypass fan model [21-23] with three rows of slot sections located one after another and united by one common cavity. A feature of the C179-2 fan stage was its high tip speed U_{tip} = 400 m/s. This led to the fact that the CT parameters to ensure simultaneous improvement of aerodynamic and acoustic characteristics of the CRTF fan with U_{tip} = 284 m/s were insufficient for improvement of aerodynamic and acoustic characteristics of the C179-2 fan model with U_{tip} = 400 m/s. Therefore, an additional correction of CT parameters is required, so that CT succeeds in improving aerodynamic and acoustic characteristics with an increase in tip speeds.

In this work, we study aerodynamic and acoustic characteristics of the C179-2 fan model with three-row CT in three modified configurations designed on the basis of the semi-empirical procedure [25].

CT of this type is characterized by the following:

- an increase in stall margin occurs without decreasing the efficiency and air consumption in the operating mode close to the design one;
- its effect increases for a fan with external disturbances;
- it increases aeroelastic stability of those rotor blades that have CTs over them;
- it reduces flow pulsations;
- it improves acoustic characteristics of fans.

3. Test object – counter-rotating fan model CRTF2A

Earlier CIAM [19,20] investigated the influence of single-row casing treatment on the noise of the ducted counter-rotating fan model CRTF2A (Figure 1). Three configurations of CT installation in the fan model casing were tested: above the first rotor, above the second rotor and above both rotors simultaneously. The positive effect of CT in relation to noise level of the counter-rotating fan model was observed when the CTs were installed above the second rotor and above both rotors; here the maximum decrease of noise level was 4-6 dB at the frequency of 2 kHz. The CT installed above the first rotor was not efficient. But the joint impact of CTs above first and second rotors resulted in noise reduction by 2-7dB within wider frequency range than in case of CT installed only above the second rotor.

This paper presents the results of studies on influence of several CT configurations on the ducted counter-rotating fan noise when CT design parameters – number of slots and cavity height – varied within the possible limits [19].

The tests were conducted with ducted counter-rotating fan model CRTF2A of 22 inches in diameter 18,26] with the casing adapted for CT installation (Figure 2).

Figure 1 – Ducted counter-rotating fan model CRTF2A – front view.

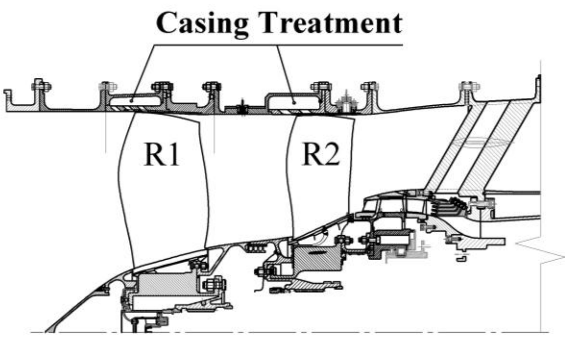

Figure 2 – Longitudinal section of fan model CRTF2A with casings.

Slot section (Figure 3) is a self-controlled CT that allows to delay the beginning of the stall processes in the compressor (fan) stage [7,8]. It assists to a normal regime of flow around the main part of the blade. The earlier studies of such CTs showed that they provide greater stall margin of fans and compressors practically without the reduction of efficiency and air flow rate at the modes close to the design one; and the efficiency of these CTs increases with the external disturbances acting on the compressor. Slot sections contributes to the higher aeroelastic stability of the blades as well and have a number of other benefits.

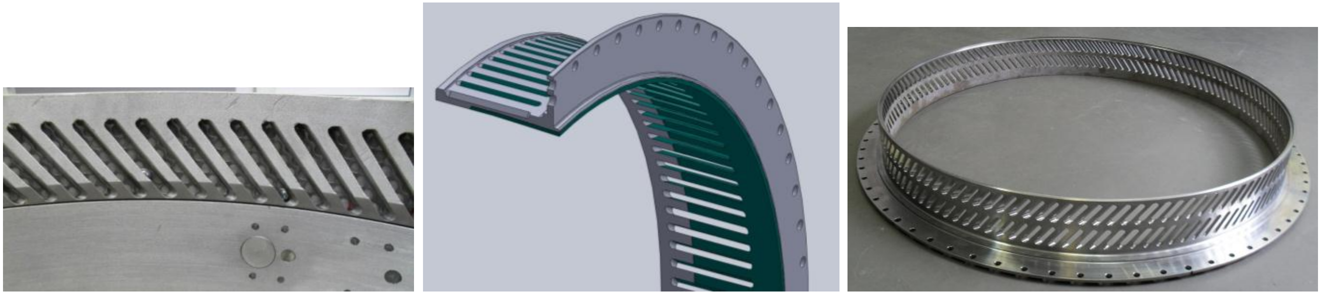

Figure 3 – Typical single-row CTs and two-row CT.

The geometric parameters of CTs are selected on the results of aerodynamic computations taking into account geometric and technological peculiarities of turbocompressors. All the geometric ratios below are interconnected and correlate with aerodynamic characteristics of stages, in particular with Mach number (M) in relative motion. According to empirical methods [3,25] of CT designing based on a great volume of experimental data, the CT design parameters were chosen.

Figures 4 and 5 show the impact of three tested CT configurations on one-third octave sound spectra of counter-rotating fan CRTF2A at “Take-off” mode.

In 90° noise emission direction (Figure 4) the fan noise is decreased within the frequency range from 2.0 kHz up to 5.0 kHz. The maximum fan noise reduction is shifted to one-third octave band with centre frequency of 4.0 kHz and reaches 12dB.

In direction of sound emission to rear semi-sphere - 120° (Figure 5) with CT installed the fan noise is decreased within the range from 1.6 kHz up to 20.0 kHz. The maximum noise reduction is observed in one-third octave band with centre frequency of 2.0 kHz and reaches the values from 9dB to 11dB, in one-third octave band with centre frequency of 5.0 kHz the noise level decreases by 6dB.

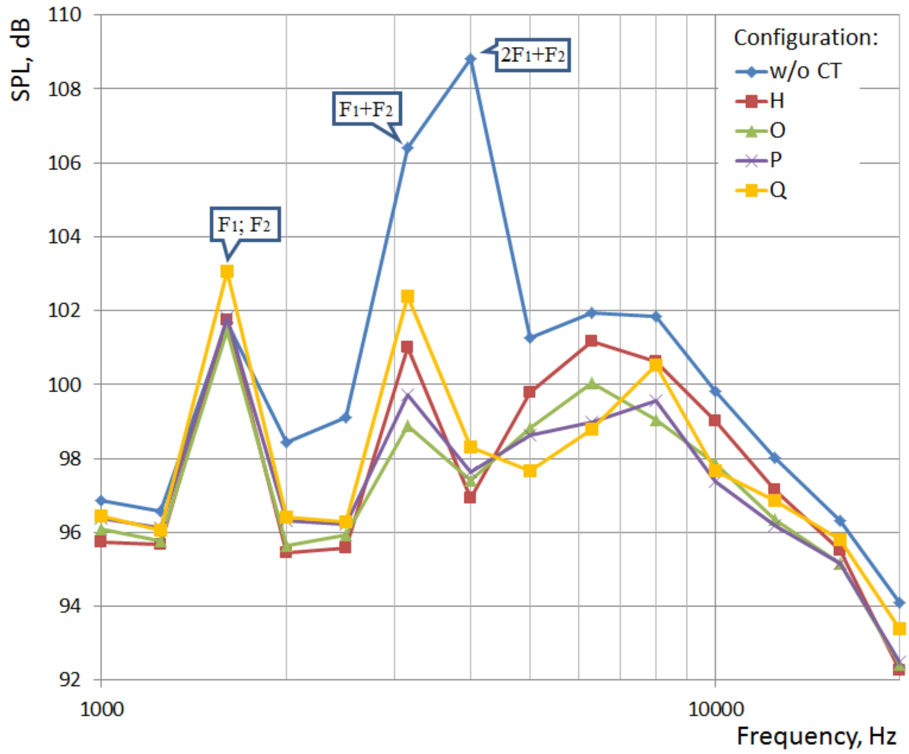

Figure 4 – 1/3-octave spectra of noise of CRTF2A with different CT configurations at take-off mode. Emission direction - 90°. Configurations H, O, P, Q. Blue line – without CT.

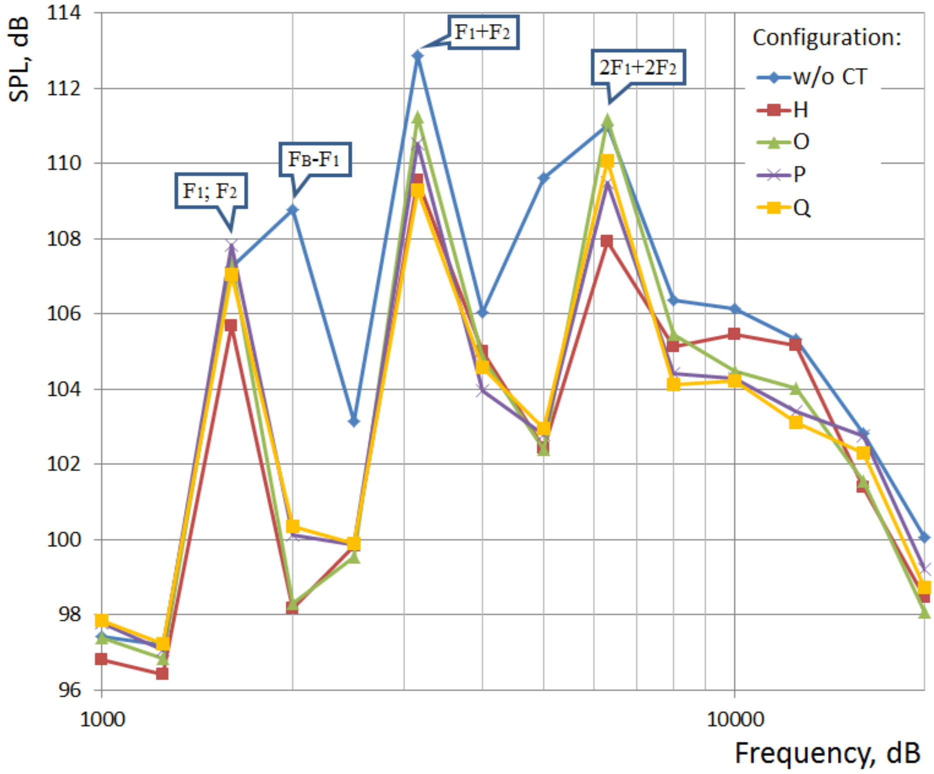

Figure 5 – 1/3- octave spectra of noise of CRTF2A with CT at take-off mode of 94%Nom. Emission direction - 120°. Configurations H, O, P, Q. Blue line – without CT.

4. Overall sound power level of counter-rotating fan model CRTF2A

For integral estimation of CT acoustic efficiency, the overall decrease in the sound power level (PWL) is used. Table 1 and Figure 6 present the main design parameters and acoustic efficiency of the tested CT configurations.

Table 1 – Acoustic efficiency of tested CT configurations, dB

Configuration designation	Acoustic efficiency of CT for different modes, dB			
	Take-off 94%N	Climb 83%N	Landing 54%N	Overall
H (Z_1=115)	2.0	0.4	0.8	3.2
O (Z_1=82; Z_2=130)	1.9	0.8	0.8	3.5
P (Z_1=130 shift; Z_2=130)	2.0	0.5	0.8	3.3
Q (Z_1=130; Z_2=130)	2.0	0.4	0.8	3.2

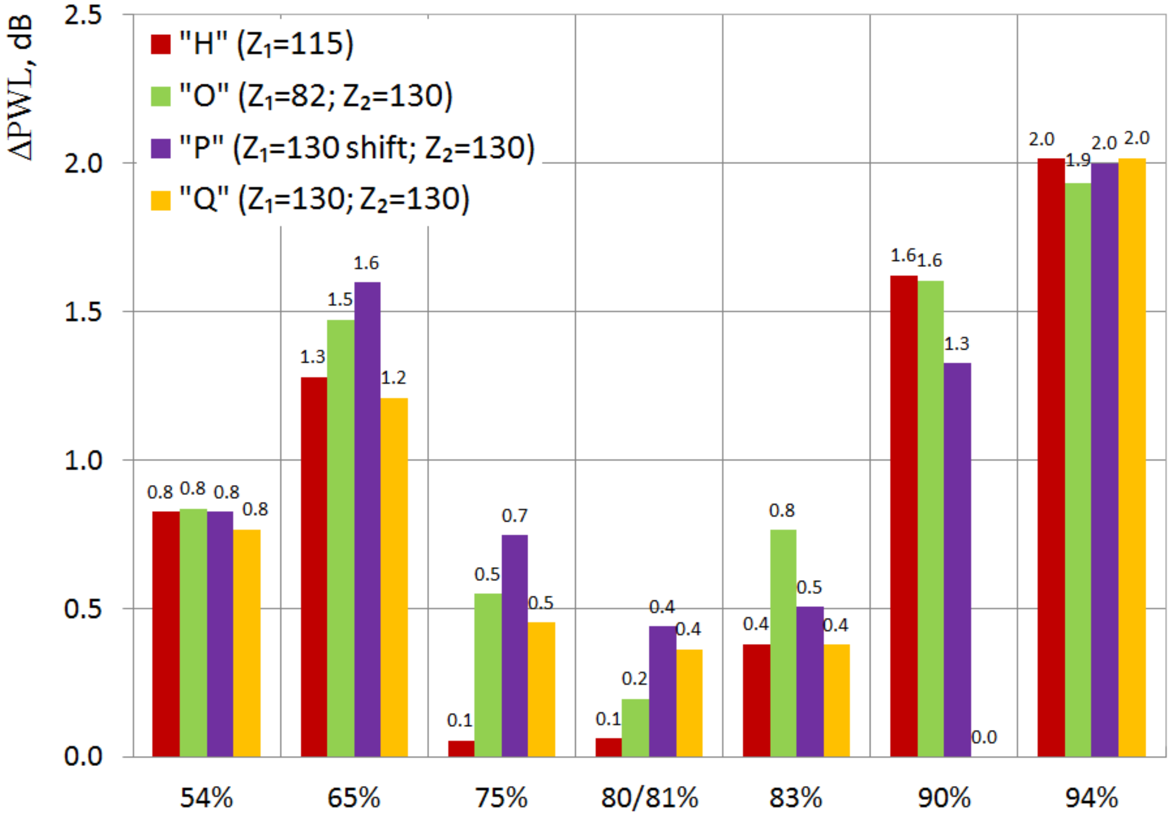

Figure 6 – Acoustic efficiency of the tested CT configurations.

Relatively high acoustic efficiency of two-row CTs was obtained at the transient modes of 65 % and 90 % Nom.

The results of experimental studies of acoustic characteristics for three two-row CT configurations showed that all three CT configurations approximately equally decrease the sound power level at three certification modes. The overall decrease in the sound power level of the fan model with two-row CT above the second rotor is from 3.2 dB to 3.5 dB. Their acoustic efficiency is approximately similar to the one of the most acoustically efficient CT configuration tested before.

5. Test object – counter-rotating fan model CRTF2A and its instrumentation scheme

The test object is a single-row bypass fan with four booster stages installed in the core duct [22-24]. The C179-2 fan model has the following geometric and functional parameters at the design point:

- diameter of the model rotor	D = 700 мм;
- total pressure ratio in the bypass duct	$\pi^*_{F\ II}$=1.4985;
- total corrected air flow	G_{cor}= 72.4298 kg/s;
- adiabatic efficiency of the bypass duct in the design mode	$\eta^*_{ad\ II}$ = 0,9166;
- total pressure ratio in LPC (fan + booster)	$\pi^*_{F\ I}$ =2,6257;
- corrected air flow in LPC	$G_{cor\ I}$ = 7,4174 кг/с;
- adiabatic efficiency of air compression in LPC	$\eta^*_{ad\ I}$ = 0.9052;
- fan bypass ratio in design mode	m=8,76;
- number of stages in the booster	K_b=4;
- corrected fan rotational speed in the design mode	n_{cor} =10550 r.p.m.

The instrumentation diagram for the C179-2 fan model with CTs in measurements of aerodynamic characteristics is shown in Figures 7-8. A vaned throttle valve is installed in the bypass duct to measure aerodynamic characteristics. For acoustic tests, a nominal nozzle (Ø= 689 mm) installed at the bypass duct outlet replaces the vane throttle valve. In addition, all measuring instruments blocking the flow passage are removed from the bypass duct.

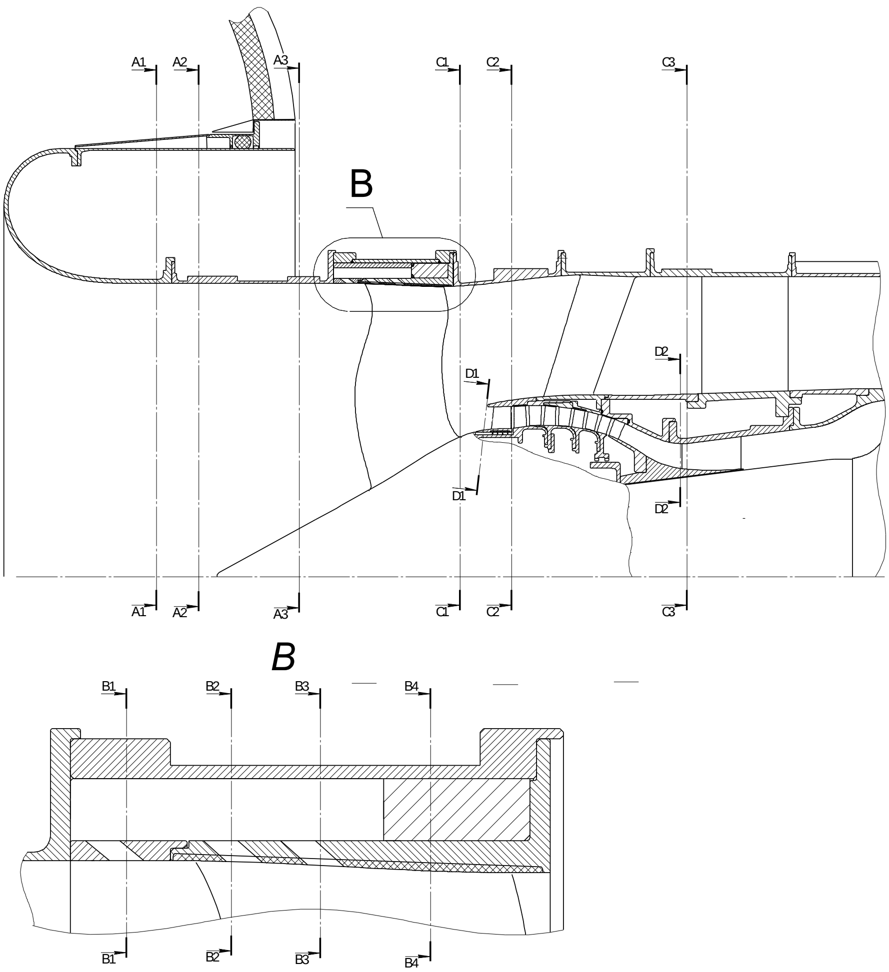

Figure 7 – General view of the C179-2 fan model with CTs and a vaned throttle valve in the bypass duct.

A2-A2
16 Ps static pressure pickups

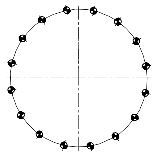

C3-C3
8 Ps static pressure pickups;
8 rakes (8x7 Pt/Tt);
1 boundary layer rake (1x8 Pt/Bl);
2 vibration pickups

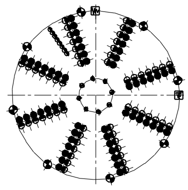

D1-D1
2 rakes (2x2 Pt/Tt), installed in IGV;
4 Ps static pressure pickups

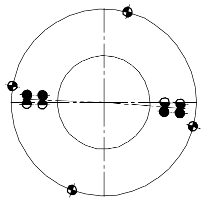

D2-D2
8 Ps static pressure pickups (4 in the bypass duct + 4 in the core duct); 4 rakes (4x4 Pt/Tt)

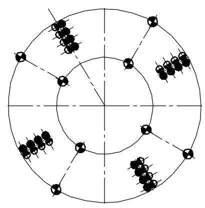

ELURA system sensor
radial clearance contact sensor
vibration pickup
traverse probe
Ps
Static pressure pulsation sensor
Pt
Tt

Figure 8 – Sections at inlets and outlets of core and bypass ducts.

6. Three-row CTs

The design of tested CTs is a combination of three rows of slots, where the number of slots in any row is chosen rather large that provides the ratio of slot width (δs) to pitch ($t_{s)}$ equal to δ_s/t_s =0.55…0.82. This choice of the design stems from results of aerodynamic computations using a semi-empirical procedure [25]. Casing treatment cavity volume is equal to 0.00267 m^3. The ratio of the blade chord at the tip to the width of the slot is equal to approximately 31.

In this series of experiments, 3 configurations of three-row CTs are used – CT No. 1, CT No. 2 and CT No. 3.

CT No. 1 has axes of slots in each row lying along the same line. The other two tested CT configurations - CT No. 2 and CT No. 3 - differ from each other in that longitudinal axes of slots of the first row in CT No. 2 coincide with respective longitudinal axes of the second row, and in CT No. 3 - with respective longitudinal axes of the third row (Figure 9).

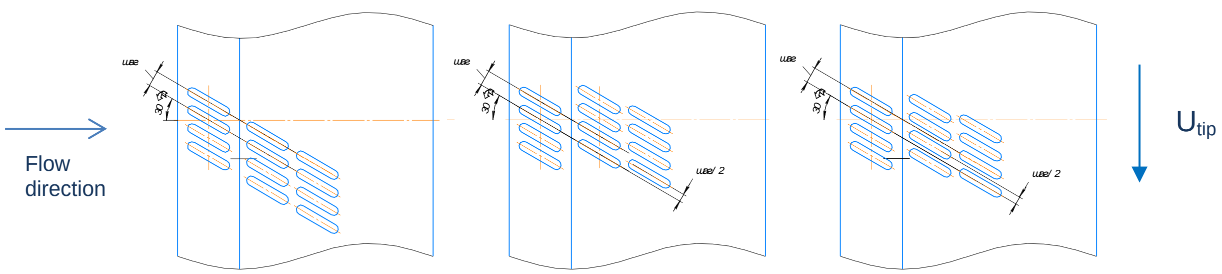

a) b) c)

Figure 9 – Relative position of slots: (a) – CT No.1 (ALL SLOTS ALONG ONE LINE); (b) – CT No.2; (c) – CT No. 3

In this series of experiments, the CT is installed over the rotor of the C179-2 single-stage fan model, as shown in Figures 10 and 11.

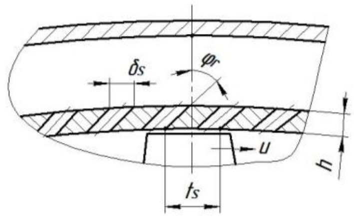

Figure 10 – Relative diagram of the fan casing fragment with CT installed over the rotor.

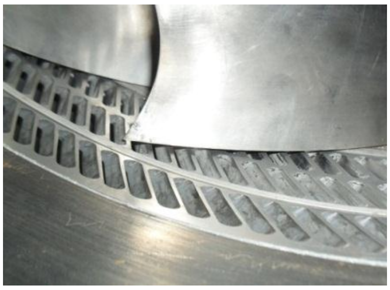

Figure 11 – Photo of CT No3.

7. Test procedures

The test object is a single-row bypass fan [21-23]. Throttle valves in bypass and core ducts are installed at the outlet the fan inner and outer flow passages. These throttles are controlled from a control room of the test facility. Therefore, operation of the single-row bypass fan is characterized by three independent parameters:

- rotor rotational speed (n);
- position of the throttle valve in the core duct (CDV%);
- position of the throttle valve in the bypass duct (BPDV%).

During aerodynamic tests, aerodynamic characteristics of the bypass duct are measured at five values of rotor corrected speeds: n=58.2%, 73.7%, 85.2%, 90.7%, and 100%.

Based on accumulated experience in tests of counter-rotating fans and single-row fans with wide-chord blades, the fan operating modes are limited not only by loss of stall margins, but by achievement of max. permissible dynamic stresses on rotor blades of the second rotor. Therefore, the leftmost points of aerodynamic characteristics of the fan under study found as a result of these tests do not match to loss of stall margins, but to max. permissible dynamic stresses in the blades. In this work, these stresses are estimated indirectly, using the “MIC DFM” proximity measuring system of vibration amplitudes in tip sections of rotor blades. In these tests, the condition is deemed as critical when the vibration amplitude of tip sections reaches 3.5 mm.

Acoustic tests are carried out with a nominal nozzle in the bypass duct at rotational speeds that correspond to approach, flyover and take-off, as well as in some interim modes.

8. Aerodynamic characteristics of the C179-2 fan model with improved three-row CTs

In this work aerodynamic characteristics for the bypass duct of the C179-2 single-row bypass fan model with a combined case treatment in three configurations are experimentally found at five values of the corrected speed: n=58.2 %, 73.7 %, 85.2 %, 90.7 % and 100 %. The leftmost points of aerodynamic characteristics correspond to maximum permissible dynamic stresses on rotor blades.

Figure 12 shows total pressure ratio in the fan bypass duct (π^*_{II}) as a function of corrected air flow in the fan bypass duct (G_{corII}) for 3 configurations of the combined CT in comparison with the initial fan configuration (without CT). As can be seen from the graphs, all CTs under study provide an increase in total pressure ratio in the left line and an increase in stall margins relative to the initial fan configuration in all operating modes.

Figure 13 shows dependences of adiabatic efficiency of the fan bypass duct ($\eta^*_{ad\ II}$) on corrected airflow in the fan bypass duct ($G_{cor\ II}$) for the same fan configurations. As can be seen from the graphs, CT No. 3 provides a steady increase in fan efficiency in all operating modes without a decrease in stall margins of the fan. In the design mode, this CT provides an increase in max. $\eta^*_{ad\ II}$ by 0.6 %. It is worth noting that in the last case, stall margin increases by 9.2 %.

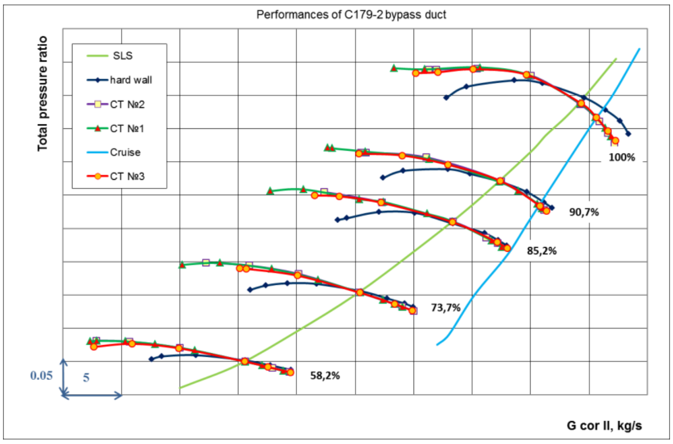

Figure 12 – Aerodynamic characteristics for the C179-2 fan with CTs.

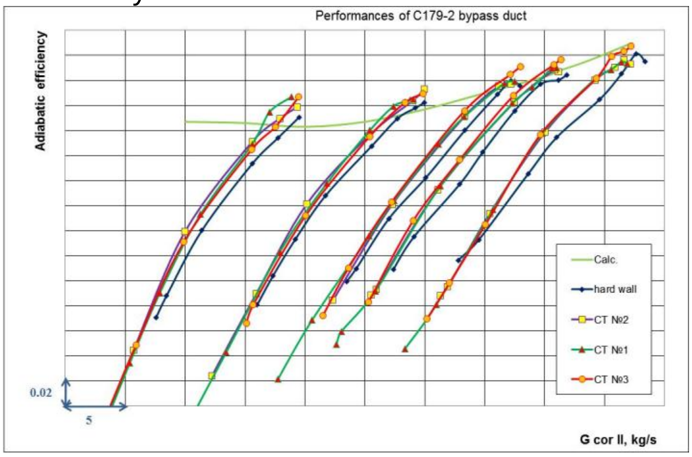

Figure 13 – Adiabatic efficiency of the C179-2 fan with CTs.

Figure 14 shows the experimentally found stall lines for the C179-2 fan with CT verses the fan in the initial configuration w/o CT. The graphs show that the CT analyzed in this series of tests provides a steady increase in stall margins in all operating modes.

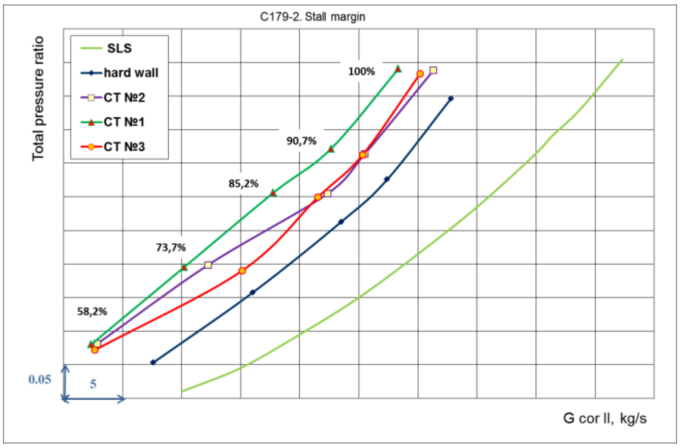

Figure 14 – Stall lines for the C179-2 fan with different CTs and without CT.

As can be seen in Figure 14, the most efficient CT No. 1 provides an increase in stall margins of the fan at low speeds (n = 58 - 74%) by 28 - 34%, at moderated speeds (n = 85 - 92%) - by 18 - 23 % and at the design point (n = 100%) - by 15%. CT No.3- the best in terms of efficiency, provides not so high increase in efficiency, but a steady increase in stall margins - by 6.4 - 9.2% within 73% <n <100% and by 30.2% at n = 58.2%. Note that in the design mode, the increase in stall margins for this CT is 9.2%.

Figure 15 shows max. adiabatic efficiency ($\eta^*_{ad\ II\ max}$) of the fan with CT as a function of the rotor speed in comparison with a similar dependence for the fan without CT. The graph shows that CT No. 3 provides a steady increase in $\eta_{*ad\ II\ max}$ of the fan under study within the total range of rotational speeds (58.2% <n <100%) by 0.6 - 1.6%, at the design point - by 0.6%, and in take-off (n = 90.7%) - by 1.3%.

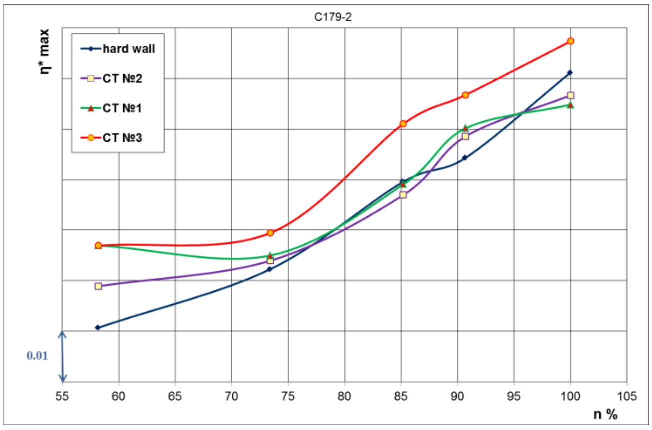

Figure 15 – Maximum adiabatic efficiency of the fan WITH different casing treatments.

9. CIAM's test facility with anechoic chamber for fan model tests

The anechoic chamber of the C-3A test facility is a 1150-m^3 rectangular room with the following linear dimensions: H = 5.0 m, L = 15.6 m, W = 14.7 m, Figure 16. The chamber walls are lined with porous sound-absorbing material (vinypore and periotex in some places). Among advantages of the C- 3A test facility are simultaneous measurements of fan noise in the front and rear hemispheres. For this purpose, a one-of-a kind shaftline was developed, which made it possible to install the fan model at a distance from the back wall equal to ten fan diameters.

The system of acoustic data collecting and processing at the C-3A test facility consist of 24 acoustic channels, each of which contains a 4939-type microphone (1/4 inch in diameter), a 2670-type pre-amplifier, AO 0416 cable (2-30 m long) and NEXSUS 2690-type four-channel amplifier. All components were manufactured by B&K company. During testing, all microphones were equipped with B&K UA 0459 anti-wind screens.

The microphones are installed in directions from 10° to 160° every 5 - 10° on two arcs with 4.0-m radius relative to the leading edge of the first rotor and the nozzle exit – see the diagram shown in Figure 16.

All measuring channels are wired to two MIK300 multi-channel recorders-analyzers manufactured by MERA company and assembled on the basis of personal computers. The multi-channel system for recording and analyzing signals transmitted by microphones was designed on the basis of M-2428 PCI boards. The operating frequency range is 0 - 100 kHz.

The software makes it possible to perform one-third octave and narrow-band analysis (maximum number of lines is 8192). The software can generate output information in ASCII format. The analyzing hardware meets the requirements of current ISO standards that apply to recording and analyzing acoustic equipment.

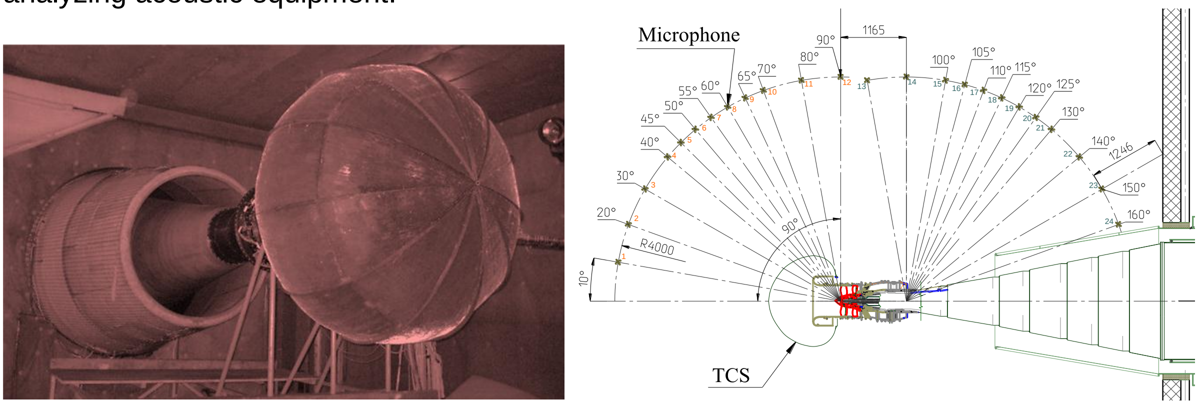

Figure 16 – Photo and location of microphones in the anechoic chamber of the CIAM's test facility.

10. Findings of experimental measurements of acoustic characteristics for the bypass fan model with CT

Studies with the aim of using the slotted CTs as "reactive" noise silencers for aircraft GTE fans have been conducting at CIAM since the 2000s [19-21]. One of the most advantageous examples of the use of CTs for this purpose is their installation over the second rotor of the counter-rotating fan. It was found that the fan noise reduction significantly depends on the design parameter defined as the ratio of the CT slot width (δs) to the CT slot cascade pitch (ts) [19-21]. The best single-row CTs in terms of fan noise suppression are characterized by a high value of this parameter equal to min. 0.6 [20].
The C179-2 single-stage fan model [22-24] was tested at rotational speeds shown in Table 2.
Table 2 – Operating modes for the C179-2 fan model

Mode	N_{cor}	N, %	BPR
58 %	6137	58.2	9.32
68 %	7173	68.0	9.28
73.7 %	7774	73.7	9.23
82 %	8277	82.0	9.17
Flyover	8987	85.2	9.16
Take-off	9735	92.3	8.83

As a criterion in estimations of CT acoustic efficiency, we use an overall decrease in the sound power level of the fan with CT installed over the rotor in take-off, flyover and approach (ΔPWL).
Figure 17 shows the comparison of one-third octave spectra of sound power density of the fan without CT and with three-row CT installed over the rotor in takeoff mode. The most noticeable change in noise levels occurs in one-third octaves with 1.25, 1.6 and 2.0-kHz central frequencies. Noise of shock waves predominates in this frequency range [22-24] and its level with CT decreases by 4 ... 10 dB. Since shock waves propagate mainly to the front hemisphere, therefore, a decrease in the noise level in the rear hemisphere in one-third octave with 1.6-kH frequency, where tonal components are absent, is indicative of the CT effect on a broadband component of fan noise (Figure 18).

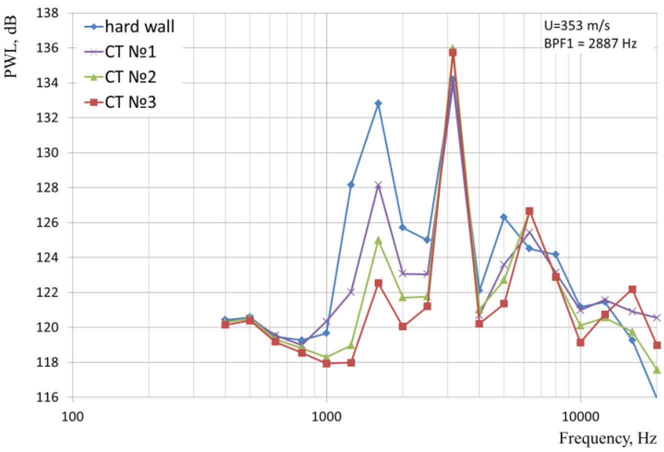

Figure 17 – One-Third octave sound power spectra for the C179-2 fan model in take- off (n= 92.3%).

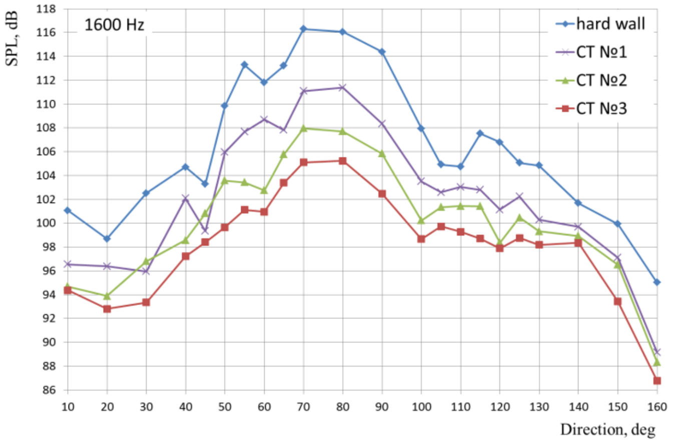

Figure 18 – Noise directivity pattern for 1.6-kHz one-third octave.

In the “flyover” mode, the CT leads to a sound power decrease in one-third octaves containing a tone at blade passing frequency (BPF1 = 2.67 kHz) and its first harmonic (BPF2 = 5.33 kHz) by 1 – 2 dB.

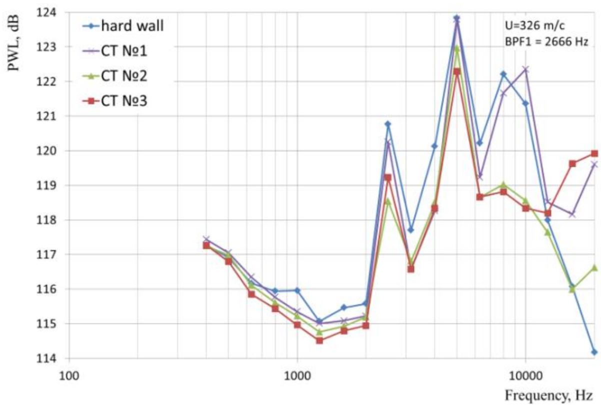

Figure 19 – One-third octave sound power spectra for the C179-2 fan model in flyover (n_{cor}= 85.2%)

Figure 19 shows an increase in the sound power level in one-third octaves with 16.0 kHz and 20.0 kHz frequencies as a result of more stronger harmonics with a high tone number at blade passing frequencies, that is BPF6, BPF7, and BPF8.

Figure 20 shows noise directivity patterns for BPF3 and BPF4. As can be seen, CT No. 3 and CT No. 2, are most efficient as noise suppressors for the second and third harmonics of tonal noise at the blade passing frequency (BPF3 = 8.0 kHz; BPF4 = 10.66 kHz). A noise decrease at these frequencies is observed in 70°-160° noise emission directions and is equal to 4-6 dB.

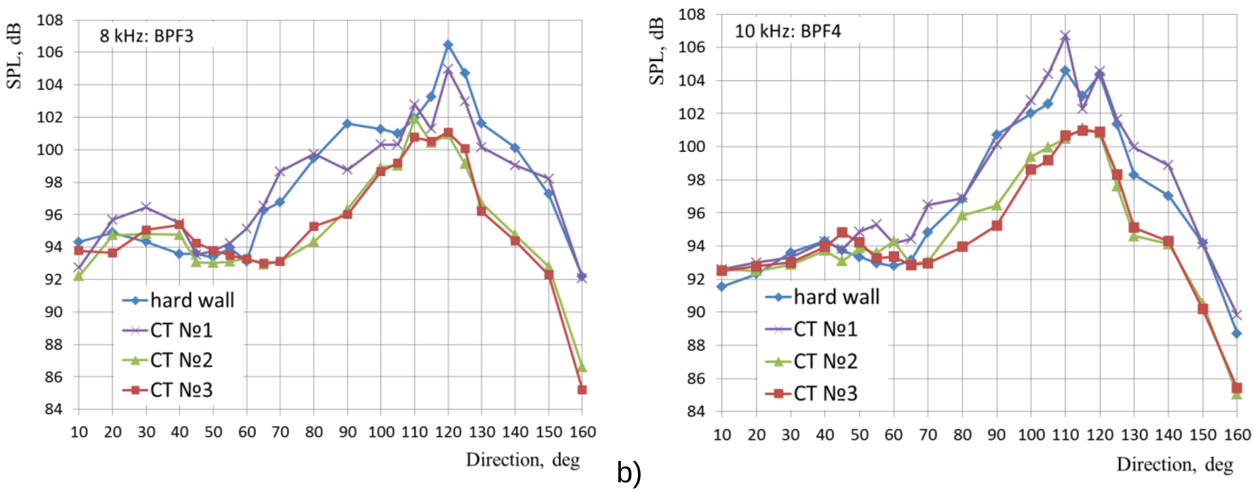

a) b)

Figure 20 – Fan noise directivity patterns: (a) at 8.0 kHz one-third octave; (b) at 10.0 kHz one-third octave

In “Approach” mode, the CT installation decreases sound power level by approx. 2 dB within the frequency range from 400 Hz to 12.5 kHz (Figure 21).

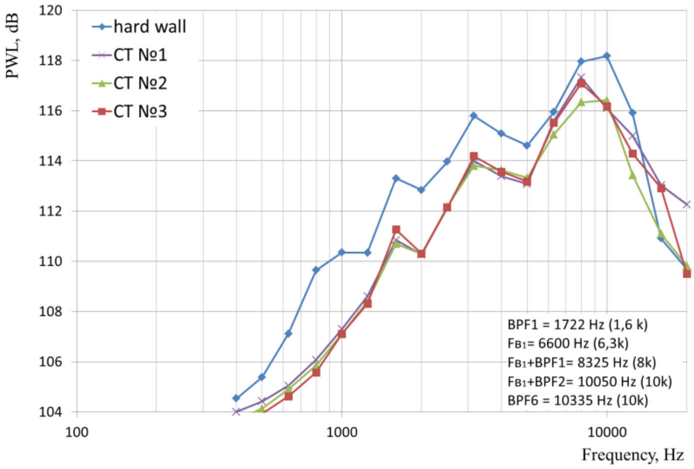

Figure 21 – One-third octave sound power spectra for the c179-2 fan model in “approach” (n= 55.0%)

Figure 22 shows total noise directivity patterns of the fan at 1600 Hz passing frequency and its first 3150-Hz harmonic. Noise reduction at high frequencies from 8 to 10 kHz is a result of attenuation of noise with BPF1 + Fb and BPF2 + Fb combination tones, where Fb is passing frequency of blades of the first booster stage in the fan.

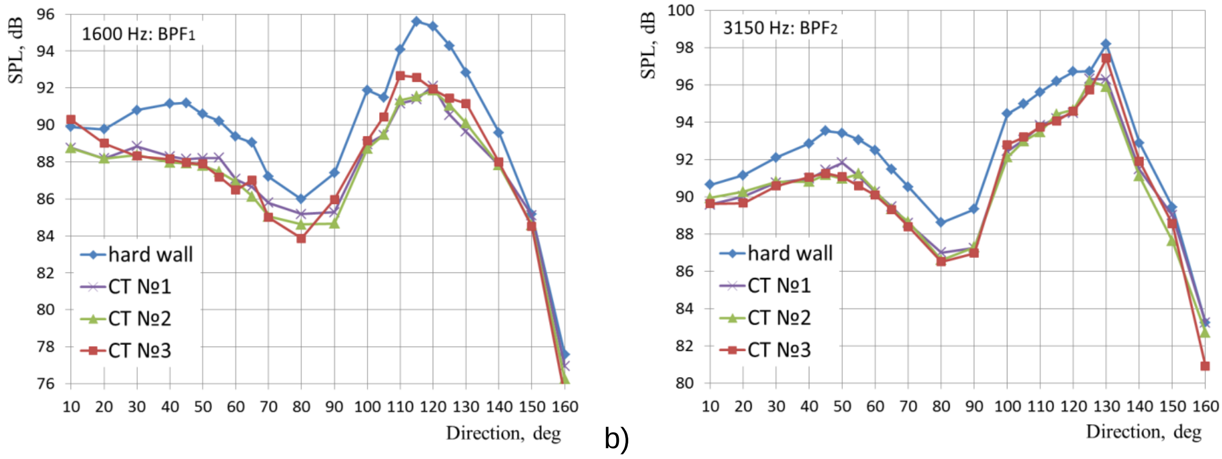

a) b)

Figure 22 – Fan tonal noise directivity patterns at a) 1.6 kHz passing frequency and b) 3.15 kHz first harmonic

The below-shown bar-graphs of overall sound power levels (Figure 23) sum up an integral criterion for assessment the impact of CTs on fan noise.

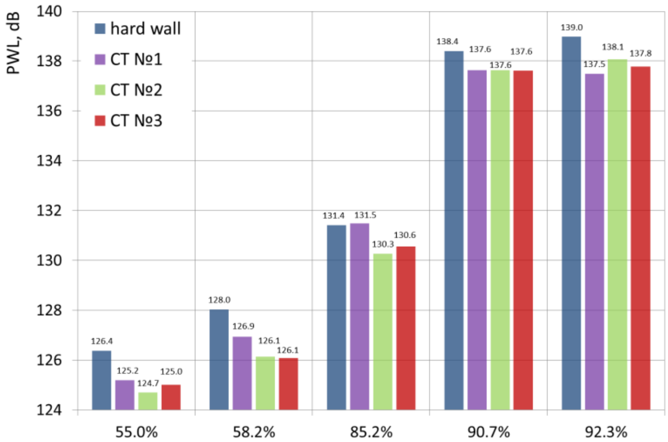

Figure 23 – Comparison of overall sound power levels of the C179-2 fan model at different rotational speeds

All three CT configurations lead to a decrease in acoustic power of the fan model in all operating modes. Table 2 shows the acoustic performance for 3 CT three-row configurations.

Table 3 – Decrease in the sound power level of the C179-2 fan model with installation of three-row CTs

CT	Operating conditions					Σ, dB (in total for 3 certification modes)
	Landing (55 %)	58,2 %	**Flyover (85,2 %)**	90,7 %	**Take-off (92,3 %)**	
No.1	1.2	1.1	-0.1	0.8	1.5	2.6
No.2	1.7	1.9	1.1	0.8	0.9	3.7
No.3	1.4	1.9	0.8	0.8	1.2	3.4

Finally, it is worth noting that according to results of experimental studies of acoustic characteristics for three-row CTs installed in the casing of the C179-2 single-stage fan and with account of three key operating modes of the fan (Take-off, Flyover and Approach), the most acoustically beneficial configurations are CT No. 3 and CT No. 2 providing a decrease in sound power by approx. 3.5 dB.

11. Conclusion

1. The results of experimental studies of acoustic characteristics for three two-row CT configurations showed that all three CT configurations approximately equally decrease the sound power level at three certification modes. The overall decrease in the sound power level of the fan model with two-row CT above the second rotor is from 3.2 dB to 3.5 dB. Their acoustic efficiency is approximately similar to the one of the most acoustically efficient CT configuration tested before.

2. To increase stall margins, improve efficiency and reduce fan noise, three versions of the casing treatment were designed and manufactured for the model stage of the C179-2 single-row bypass fan.

3. Three CT versions were experimentally studied as applied to the C179-2 single-row bypass fan.

4. Based on the analysis of experimental data, the following findings were achieved:

- all studied CT modifications provide an increase in pressure ratio in the left line of the characteristic and an increase in stall margins of the fan in all operating conditions (n = 58 – 100 %);

- CT No. 1 provides an increase in stall margins in low operating modes (n = 58 – 74 %) by 28 – 34 %, in medium modes (n = 85 – 92 %) - by 18 - 23% and in the design mode (n = 100%) - by 15%;

- CT No. 3 provides a concurrent increase in fan efficiency and stall margins in all operating modes. Max. efficiency increases by 0.6 - 1.6 %, stall margin increases by 6.4 - 9.2 % at $73\% < n < 100\%$ rotational speeds and by 30.2% at n = 58.2 %;

- as a result of analysis of total pressure ratio and efficiency at the fan outlet with various types of casing treatments, it is found that CT No. 3 provides the best efficiency in the flow core.

5. Based on experimental studies of acoustic characteristics of CTs installed in the casing of the C179-2 single-stage fan for three key operating modes of the fan - "Take-off", "Flyover " and "Approach" - the most acoustically efficient are CT No. 3 and CT No. 2 providing a decrease in sound power by approx. 3.5 dB.

12. Contact Author Email Address

The contact author email address: vimileshin@ciam.ru

13. Copyright Statement

References

[1] F.S. Gelmedov et al., Russian Federation*, "ANTI-STALL TIP TREATMENT MEANS", United States Patent # 5,762,470* June 9, 1998.
[2] *F*.S. Gelmedov, E.A. Lokshtanov, L.E. Olshtein, M.A. Sidorkin, Russian Federation, *"ANTI-STALL TIP* TREATMENT *MEANS", European Patent specification # EP 0688 400 B1,* 1997.
[3] V.I. Mileshin*. "Numerical and experimental investigation of bypass fan stage models and high loaded compressor* stages *for development of new fan and high pressure compressor for advanced engines". Key-note speech at 10th European Turbomachinery Conference ETC10, April 15-19 2013, Lappeenranta, Finland,* 2013.
[4] V.I. Mileshin. *"Challenges in fan and high pressure compressor development". Key-note speech at XXI International* Symposium *on Air Breathing Engines ISABE 2013, September 9-13, 2013, Busan, Korea,* 2013.
[5] Victor Mileshin, Igor Brailko and Andrew Startsev, *"Applications of Casing* Circumferential *Grooves to Counteract the Influence of Tip Clearance", ASME paper, GT2008-51147,* 2008.
[6] Xi Nan, Feng Lin, Juan Du, Jingyi Chen*. "The Momentum Balance in the Blade Tip Region and The Effectiveness of Circumferential Grooves in a Transonic Rotor". Proceedings of GT2013 ASME Turbo Expo, June 3-7, San Antonio, USA, GT2013- 95372,* 2013.
[7] M. Hembera*. "Simulation of casing treatments of a transonic* compressor *stage". International Journal of Rotating Machinery, 2008, Article ID 657202,* 2008*.*
[8] I. Wilke and H.-P. Kau. *Stall margin enhancing flow mechanisms in a* transonic *compressor stage with axial casing slots. The 10th* of *International Symposium on Transport Phenomena and Dynamics of Rotating Machninery, 10-2004-006,* 2004.
[9] C. Brandstetter, J. A. Streit, F. Wartzek, F. Heinichen, H.-P. Schiffer *"An Advanced Axial-Slot Casing Treatment on a Tip-Critical Transonic Compressor Rotor Part 1: Unsteady Hot Wire and Wall Pressure Measurements". Proceedings of10th European Turbomachinery Conference ETC10, April 15-19 2013, Lappeenranta, Finland, Paper 068,* 2013.
[10] J. A. Streit, C. Brandstetter, F. Heinichen, H.-P. Kau. *"An Advanced Axial-Slot Casing Treatment on a Tip-Critical Transonic Compressor Rotor Part 2: Taking a Closer Look With CFD". Proceedings of10th European Turbomachinery Conference ETC10, April 15-19 2013, Lappeenranta, Finland, Paper 070,* 2013.
[11] Chuhill HAH, Martin MUELLER, Heinz-Peter SCHIFFER. *"Study on Convective Flow Effects in Endwall Casing Treatments in Transonic Compressor Rotors". Proceedings of GT2012 ASME Turbo Expo, June 11-15, Copenhagen, Denmark, GT2012-68411,* 2012.
[12] *Chen, H.,* Huang*, X., Shi, K., Fu, S., Bennington, M.A., Morris, S.C., Ross, M.,* McNulty*, S., and Wadia, A., 2010, "A CFD Study of Circumferential Groove Casing Treatments in a Transonic Axial Compressor," ASME Paper GT2010-23606,* 2010.
[13] Crook, A. J., Greitzer, E. M., Tan, C. S., and Adamczyk, J. J., *"Numerical* Simulation *of Compressor Endwall and Casing Treatment Flow Phenomena," ASME Journal of Turbomachinery, Vol. 115, No. 3, pp. 501-512,* 1993.
[14] Fujita, H. and Takata, H., *"A Study of Configurations of Casing Treatment* for *Axial Flow Compressors," Bull. of ASME, Vol. 27, No. 230, pp. 1675-1681,*1985.
[15] Hah, C., Rabe, D. C., and Wadia, A. R., *"Role of Tip-Leakage Vortices and Passage Shock in Stall Inception in a Swept Transonic Compressor Rotor," ASME Paper GT2004-53867,* 2004*.*
[16] Talbotec, J.; Vernet, M. Snecma counter rotating fan aerodynamic design logic & tests results. In Proceedings of the 27th International Congress of Aeronautical Sciences, Nice, France, 19–24 September 2010; ICAS2010-087, 2010.
[17] Cailleau, J.-M. CRTF fan aerodynamic & Acoustic design & concept improvement - Preliminary results. In Proceedings of the VITAL Workshop, Budapest, Hungary, 9–10 March, 2009.
[18] Khaletskiy, Yu.; Mileshin, V.; Talbotec, J.; Nicke, E. Study on Noise of Counter Rotating Fan Models at CIAM Anechoic Chamber. In Proceedings of the 28th International Congress of Aeronautical Sciences, Brisbane, Australia, 23–28 September 2012; Paper ICAS2012-897, 2012.
[19] Khaletskii, Iu, Mileshin, V. Experimental study of casing treatment impact on ducted counter-rotating fan noise. In Proceedings of the 22nd International Congress on Acoustics, Buenos Aires, Argentina, 5–9 September 2016; ICA2016-0108, 2016.
[20] Khaletskii, Iu, Mileshin, V, Korzhnev, V, Pochkin, Ya. Influence of the casing treatment design parameters on the ducted counter rotating fan noise. In Proceedings of the 24nd International Conference on Sound and Vibrations, London, UK, 23–27 July 2017; ICSV-364, 2017.
[21] *Mileshin V.I.,* A Review of New Experimental Technologies for the Development of Advanced Fans with High Bypass Ratio, *International Journal of Turbomachinery Propulsion and Power.* Int. J. Turbomach.

Propuls. Power **2018**, 3(3), 21; doi:10.3390/ijtpp3030021, *www.mdpi.com/journal/ijtpp*, 2018.

[22] S.V. Pankov, V.I. Mileshin, I.K. Orekhov. Numerical and experimental investigations of single-flow and bypass-flow fans. *FAN 2012-39,* Senlis (France), 18-20 April, 2012.

[23] Pankov S., Mileshin, V.; Korzhnev, V., *Numerical and Experimental Investigations Bypass-Flow Fans for an* Advanced Civil *Aircraft Engine. In Proceedings of the 28th International Congress of Aeronautical Sciences, St. Peterburg, Russia, 7-12 September 2014; Paper ICAS2014-0104,* 2014.

[24] V.N. Korzhnev, V.I. Mileshin, S.V. Pankov. Numerical and experimental investigations of bypass flow fan for an advanced civil aircraft engine. TsAGI Science Journal. 2019. T. L, № 3. p. 3-18.

[25] Gelmedov, F.Sh.; Mileshin, V.I.; Kozhemyako, P.G.; Orekhov, I.K. Stall margin improvement in three-stage low pressure compressor by use of slot type casing treatments. *Proceedings of the ASME Turbo Expo 2014*, Düsseldorf, Germany, 16–20 June 2014; GT2014-26298, 2014.

[26] V.I. Mileshin, S.V. Pankov, V.A. Fateev "Ducted Counter-Rotating Fan Blades Optimization Based on 3D Inverse Problem Solution aiming at fan gasdynamics improvement". *Proceedings of ISABE Conference*, Paper ISABE2009-1334, Montreal, Canada, 2009.